International Journal of Disaster Risk Reduction xxx (xxxx) xxx–xxx

Contents lists available at ScienceDirect

International Journal of Disaster Risk Reduction

journal homepage: www.elsevier.com/locate/ijdrr

Modeling fire spread in cities with non-flammable construction

Yonatan Shaham[a,b,*], Itzhak Benenson[a]

[a] Department of Geography and Human Environment, Tel Aviv University, Tel Aviv, Israel
[b] Porter School of Environmental Studies, Tel Aviv University, Tel Aviv, Israel

ARTICLE INFO

Keywords:
Fire modeling
Non-flammable construction
Geosimulation
Emergency preparedness
Arid climate

ABSTRACT

City-scale models of urban fires were developed for countries where most construction is highly flammable, such as the US, China and Japan. Essential adjustments of existing models are required for modeling fire spread at the city scale in urban areas where construction is non-flammable and the space between buildings is filled by flammable vegetation, as in Mediterranean and Middle Eastern cities. We develop a spatially explicit city-scale model of urban fire spread for cities consisting of non-flammable buildings and apply it to different areas of the city of Haifa, Israel. We demonstrate that adequate modeling of fire spread inside non-flammable buildings demands accurate partition of the intra-building space into apartments and corridors. We present and evaluate the algorithm for establishing such partition based on standard GIS layer of the buildings footprints.

Based on the model, we demonstrate that fire spread in cities consisting of non-flammable buildings is highly sensitive to the structure of urban vegetation within the immediate surroundings of each building and investigate the effects of vegetation management policies on fire spread mitigation. We discuss the use of the model for establishing the procedures of firefighters' response during routine and multiple ignition scenarios.

1. Introduction

A city's preparedness to fires demands spatially explicit and properly validated city-scale modeling of fire spread. Such models allow to produce fire risk maps and to establish fire management procedures, as well as to prioritize firefighters' response to a wide spectrum of weather conditions. City-scale urban fire spread models include sub models of two basic processes: fire spread within a building, and fire transmission between buildings. Recently, several successful simulation models of city-scale urban fires were proposed for the US, Japan and China [1–3], where most buildings are flammable. These models are based on controlled indoor fire experiments and were validated against well-documented examples of city-scale fires.

However, the existing models are developed for cities of flammable buildings and cannot be applied to those parts of the world where buildings are typically constructed from non-flammable materials. The latter is characteristic of Mediterranean and Middle-Eastern (MME) cities. In addition, in MME cities the inter-building space is often filled with vegetation that, in the summer, is dry and very flammable. In these circumstances, the basic sub-models of fire spread in the building and between buildings and the entire model of fire spread in the city should be reconsidered.

In this paper we develop a city scale fire spread model for a city of non-flammable buildings (NF-cities) and validate and investigate this model in the city Haifa, Israel. Our goal is to identify the patterns of fire spread and estimate risks of fire expansion for fires that may start in any building in the city. Such city-wide analysis of fire risk at the fine scale of a single building is necessary for assessment of urban resilience and facilitating long-term mitigation efforts and real-time response. We, thus, intensively use urban GIS and aerial photography. In addition, modeling fire spread in non-flammable building demands realistic partitioning of each floor into rooms, apartments and corridors. For this purpose, we develop a novel building's footprint partitioning (FP) algorithm.

1.1. Existing city-scale models of fire spread

Fire spread in cities should be considered in two levels: the first level concerns the development of a fire inside a building, and the second levels concerns fire spread between buildings. At both levels, the dynamics of fire, in time and space is determined by the spatial patterns of fuel and fire-controlling factors. Indoor fires develop in conditions where oxygen is limited and therefore critically depends on the ventilation conditions defined by the building architecture. Outdoor fires are not limited by the oxygen and are mostly controlled by the atmospheric conditions and the type and spatial pattern of the outdoor fuel.

Several modeling approaches for fire development within a building are well accepted: computational fluid dynamics models [4,5], "zone"

* Correspondence to: Porter School of Environmental Studies, Tel Aviv University, P.O. Box 39040, Tel Aviv 6997801, Israel.
E-mail addresses: yjonas83@gmail.com (Y. Shaham), bennya@post.tau.ac.il (I. Benenson).

https://doi.org/10.1016/j.ijdrr.2018.03.010
Received 7 November 2017; Received in revised form 4 March 2018; Accepted 5 March 2018

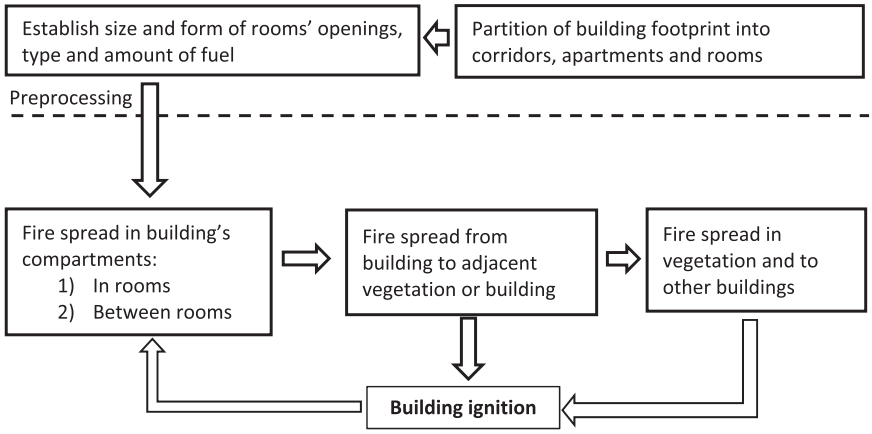

Fig. 1. General scheme of the model of fire spread in the NF-city.

models [2,6,7] and "parametric" models [8,9]. All these approaches consider five mechanisms of fire transmission between rooms and apartments inside a building and between buildings: (1) burn through walls and ceilings, (2) direct ignition by flame impingement (through doors and windows) (3) direct ignition from nearby burning vegetation, (4) heat radiation from flames and gas, and (5) firebrands [1–3,10]. The effectiveness of each of the mechanisms varies greatly with respect to location-specific conditions, even at the scale of few meters.

Computational fluid dynamics models investigate a set of partial-differential equations that express the laws of local conservation of mass, momentum, energy, and gases in a continuous space [4,6]. Zone models use a similar approach but divide the modeled space into a specific set of distinct "zones" in each built compartment, such as a room or a corridor: a zone of lower layer of gases with relatively low temperature, a zone of upper hot layer of gases with relatively high temperature, the envelope of the fire compartment (room, hallway etc.) and its openings [2,6].

Parametric models relate between physical parameters of construction, dimensions of fire compartment, dimensions of compartment's openings, and fuel type and density. They use a set of empirically verified non-linear regressions to represent heat release rate, mass lose rate of burning fuel, and time-temperature dependency [1,8,9].

Himoto and Tanaka [2] developed and applied a zone model for Japanese cities, based on explicit representation of heat transfer using thermodynamics equations. A study by Zhao [3] is focused on Chinese cities with flammable construction. Zhao's model uses the parametric approach, using typical durations of burning phases and temperatures as dependent on building type and size, to calculate fire spread within buildings, and uses the work of Himoto and Tanaka [2] to model building-to-building fire spread. Finally, Lee and Davidson [1] used a detailed parametric fire spread model to develop a model for California, US. A later work by Li and Davidson [10] expands the model to include fire spread through urban vegetation.

Parametric models are the majority among the city-scale fire spread models [10], since most of their parameters can be estimated based on the available data and their forecasts fit well to the real-world observations [1,3]. In this paper, we follow this approach and develop a parametric model of fire spread in NF-cities that continues the line established in [1,10]. To adequately represent fire spread in the building, we propose a novel algorithm of partitioning buildings' footprint into apartments, rooms, and corridors.

The rest of the paper is as follows: Methodological Section 2 presents the major characteristics of cities of non-flammable buildings, the adjusted fire spread model and the major steps of the novel FP algorithm of intra-building partitioning that is necessary for applying the model. Section 3 describes our case study of Haifa, Israel. Section 4 presents the results of the model application. We conclude the paper with a discussion of model's implications for urban-fire preventing policy. The equations of the fire spread model in the city of non-flammable buildings are given in Annex A, and the full algorithm of a building's footprint partition into rooms, apartments and corridors is given in Annex B.

2. Methods

2.1. NF-cities characteristics

NF-cities have two basic characteristics that are important for representing fire dynamics: (1) the majority of construction is non-flammable, usually made of blocks of concrete or other non-flammable material, (2) to decrease summer heat pressure, large parts of the space between buildings is filled with planted vegetation which becomes highly flammable in the summer and autumn. As a result, (1) fire cannot burn through the non-flammable walls and ceilings, and the buildings' internal partitioning may have a major effect on fire spread. (2) Non-flammable roofs reduce the effects of radiation and brands creation. Thus, the danger of fire transmission between buildings by direct ignition or radiation is relatively low, while ignition of the urban vegetation between buildings through windows and brands becomes a major factor of fire spread.

2.2. General scheme of the fire spread model

Our model of fire spread in the NF-cities follows the parametric approach and extends the models proposed by Lee, Li and Davidson [1,10] in several respects.

The first is a new algorithm of floor partition into rooms, apartments, and corridors as well as explicit allocation of doors and windows.

The second is a new description of the fire transmission between buildings and vegetation and fire spread within the vegetation. We employ an explicit description of fire transmission mechanisms, of ignition by direct contact and radiation along with an explicit use of the vegetation fire spread models.

The general structure of the model is presented in Fig. 1. At the preprocessing steps, the buildings' footprints are partitioned using the new partition algorithm (see Section 2.4.2.). Then the fire spread is calculated accounting for direct ignition, radiation, and fire brands. In case vegetation is ignited, fire spread in vegetation is calculated based on vegetation type and meteorological conditions.

The model of urban fire in the NF-city is implemented with the GAMA simulation platform [11] and is available for the download at https://github.com/YonatanShaham/MME_fire. In what follows we describe model's components in details.

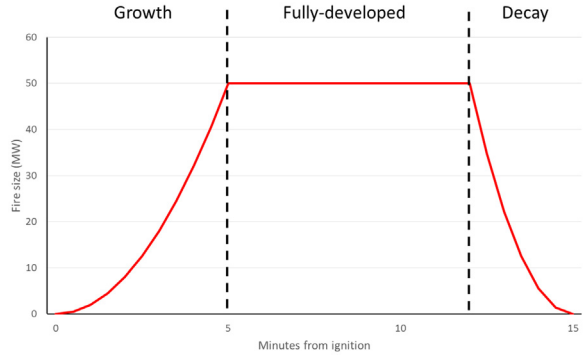

Fig. 2. Typical fire development inside a room, with burning phases.

2.3. In-room fire development

Just like Lee and Davidson [1], we follow the parametric fire model proposed by Law [12], and Law and O'Brien [13] for the description of fire development within rooms as dependent on ventilation regime, the inflow of oxygen, and the exhaustion of fire products there. The model's parameters are the type and amount of fuel, the dimensions of walls, floor and ceiling, the size and position of rooms' openings, wind direction and speed (see Annex A for the complete set of equations). The model predicts the rate of fuel burning ($\dot{m}_r$, measured in kg/s), which further defines the timing and temperature of three phases of fire development: fire growth, steady fully-developed fire, and decay (Fig. 2). Following [1] we assume that the fully-developed phase starts when 30% of the fuel is consumed, and the decay phase starts when 80% of the fuel is consumed.

Fire behavior in the room is highly sensitive to its ventilation regime. In the extreme case the wind blows though the room, entering from one window and exiting from another, and thus oxygen supply is maximal ('through-draft' conditions) and burn rate is faster. Following Lee and Davidson [1], our model ascribes through-draft conditions when the wind speed is above 5 m/s and windows are located such that the wind enters through one window and exits through the other.

To validate the Law and O'Brien's [13] model for non-flammable rooms, we compare their predictions to the experimental data on fire development in non-flammable rooms obtained much later by Lennon and Moore [14] who present time-temperature curves for 8 full-scale experimental fires in large rooms built from concrete blocks. Lennon and Moore [14] explored three factors that can influence fire development in the room: number of openings in the room – one or two, wall linings – standard or highly-insulating, and two types of the fuel load in the room: wood-only load of 40 kg/m^2, and mixed wood and plastic fuel load with energetic content equal to the wood load.

The model outputs and Lennon and Moore's [14] experimental data on burning phases' durations and temperatures are presented in Table 1. We group the eight experiments into two groups: rooms with one opening and rooms with two opening. The reason is that city-scale data on building materials and specifics of fuel content is not available in most cases, while data on the configuration of openings (i.e., windows) can be generated from a simple field survey and a partitioning algorithm (partitioning algorithms are discussed in detail in Sections 2.4.2, 2.4.3.).

As can be seen, in the case of one window, the fit between the model outputs and the experiment is very good and the differences are statistically insignificant at p ~ .5. In case of two openings, the duration of burning phases in the model is essentially and significantly (at p = 0.05) longer in the model than in the experiment. Faster fire development in two-window experiments can be explained by emerging through-draft conditions that accelerate fuel burning: non-uniform distribution of fire in the non-flammable room can cause cold air with high oxygen concentration to enter through one window and hot gases to exhaust through another, creating relatively fast air flow, high oxygen supply and faster burn rate. Such through-draft conditions are not likely in the case of flammable rooms, where burning walls and ceiling result in many holes in the room's envelope and where air flows from and into many directions.

According to Table 1, fire development in the experiments in the room with two openings is 1.7 faster than in the model. To account for this fact in the model experiments we increase the burning rate ($\dot{m}_r$) of the fuel in the room with two windows 1.7 times (see Eq. (2) in Annex A). This change accelerates burning but does not influence other aspects of fire dynamics.

Note that modeled temperature is always ~100° higher than in the experiments (Table 2). The potential effect of this difference is a slight increase of fire spread by radiation in the model. Since the goal of our model is to facilitate preparedness, we chose a conservative approach and, in the simulations below, we exploit the higher value of temperature, as generated by the model.

2.4. In-building fire development

2.4.1. In-building fire spread

In Lee and Davidson's model [1], fire spreads to adjacent and upper rooms by burn-through of flammable walls and ceilings. This mechanism is impossible in the NF-city and we thus exclude it from the model.

Two mechanisms of direct ignition during the fully-developed phase are accounted for in describing fire spread between rooms: burn through doors and burn by the flames impinging from windows.

Burning through doors: In the Lee and Davidson [1] model the spread of fire through doors is dependent on whether the door is open. In NF-cities internal doors are highly flammable, and we thus assume that fire spreads through doors irrespective of whether the door is closed or open and that rooms connected by doors to the burning room are ignited immediately, when a fire in an original burning room reaches the fully developed phase.

Flames impingent from windows and direct ignition of adjacent windows: this mechanism is effective when the fire reaches the fully-developed phase. Flames impinging from windows touch windows of other rooms and ignite windows' frames and in-room fuel immediately. Geometry and temperature of impinging flames are calculated using empirical equations drawn from the experiments described in [13,15], see Annex A for detailed equations. The parameters that define flame dimensions are in-room fire temperature, geometry of openings and wind speed. According to [13,15] for the through-draft conditions, flames are ejected only from the downwind windows and their geometry is flatter and longer than during non-through-draft conditions.

Table 1
Comparison between the model outputs and experimental full-scale fires of Lennon and Moore [14].

	One opening		Two openings	
	Model output	Average, SD for four experiments	Model output	Average, SD for four experiments
Time to the beginning of fully developed phase (MM:SS)	12:55	13:20 (4:42)	13:45	7:30 (2:30)
Time to the end of fully developed phase (MM:SS)	32:27	33:20 (4:42)	36:40	26:15 (4:09)
Average temperature during fully developed fire (C)	1413	1322 (24.4)	1437	1343 (7.7)

The parallel phenomenon of ignition of the adjacent vegetation by impinging flames is addressed in Section (2.5.3.) below.

2.4.2. Establishing buildings' internal partitioning

Fire spread in a building is critically dependent on the floors partition into apartments and rooms and location of doors and windows. This information is usually absent from the standard urban GIS database that typically contains a layer of buildings' footprint and height. To overcome this problem, Lee and Davidson [1,16] proposed a simple algorithm of partitioning a buildings' footprints into square rooms connected by doors with a window in each outer wall of the room (Fig. 3a). The algorithm was applied to the layer of buildings' footprints in the town of Grass Valley, California, and the resulting partition was part of a successfully validated simulation of the well-documented 2007 fire there [10].

In cities with flammable construction such as in California, the buildings' walls and ceilings comprise a large portion of the available fuel load, and the partition of a floor into rooms may be thus less important. The situation is different in cities of non-flammable buildings, where exact knowledge of the floor's internal partitioning into rooms, apartments and corridors and the locations of the openings is critical for describing the fire spread in the building. The corridors may be especially important as they are usually empty of fuel and separated from apartments by metal doors [17] and may essentially slow fire spread. We thus propose a new FP-algorithm for the partitioning of the building's footprints into apartments, rooms and corridors. The algorithm is especially focused at residential and regular office buildings with their standardized internal division. It may be less applicable to commercial or public buildings. Below we present the major steps of the algorithm (Fig. 3b–e). Full description is given in Appendix B. In addition to the building footprint, the FP-algorithm exploits typical room size and typical apartment size in the area (parameters of the algorithm) that can be estimated based on the buildings plans or using surveys.

Step 1: Construct minimal rectangle that contains building's footprint

a) Establish a minimal bounding rectangle, which long side is parallel to the longest dimension of the building. Set the long side that is closer to the nearest road as building's "facade"
b) Divide minimal bounding rectangle into a grid of square cells of a typical room size. Merge partial cells with the adjacent full cells (Fig. 3c).

Step 2: Create entrances and corridors

a) Consider groups of 5 cells along the "facade." Residual cells are considered as a special case (see Appendix B). If this is a ground floor set an entrance door in an outer edge of a third cell among each five and establish a corridor by merging an entrance cell with all cells after it in the perpendicular to the façade direction, except the last one (Fig. 3d). Number entrances as 1, 2, 3, …
b) At the higher floors start the corridor from the 2nd cell after the entrance, so the corridor will not include outer cells (Fig. 4)

Step 3: Establish apartments and windows

Accumulation of rooms to apartments:

a) Start with the outer cell at the left of the entrance and follow the outer ring of rooms.
b) Follow the outer ring and accumulate rooms to the apartment until the total floor area of the accumulated rooms exceeds half of a typical floor area of apartments in the study area. Then start a new apartment.
c) After all rooms in the outer ring are assigned to apartments, assign rooms of the inner ring: add each room of the inner ring to the apartment that has the largest number of rooms of the outer ring that are adjacent to this room. If the number of adjacent rooms is the same for two or more apartments, assign the room to the apartment with the smaller floor area.

Create windows:

a) Create windows in the outer walls according to wall length (typically one per outer wall of a room, see Annex B).

Step 4: Establish doors (Fig. 3e).

a) For each apartment, create one non-flammable door to adjacent corridor. If there is no such corridor, create the door in the outer wall of the building.
b) Create flammable doors between all adjacent rooms of the same

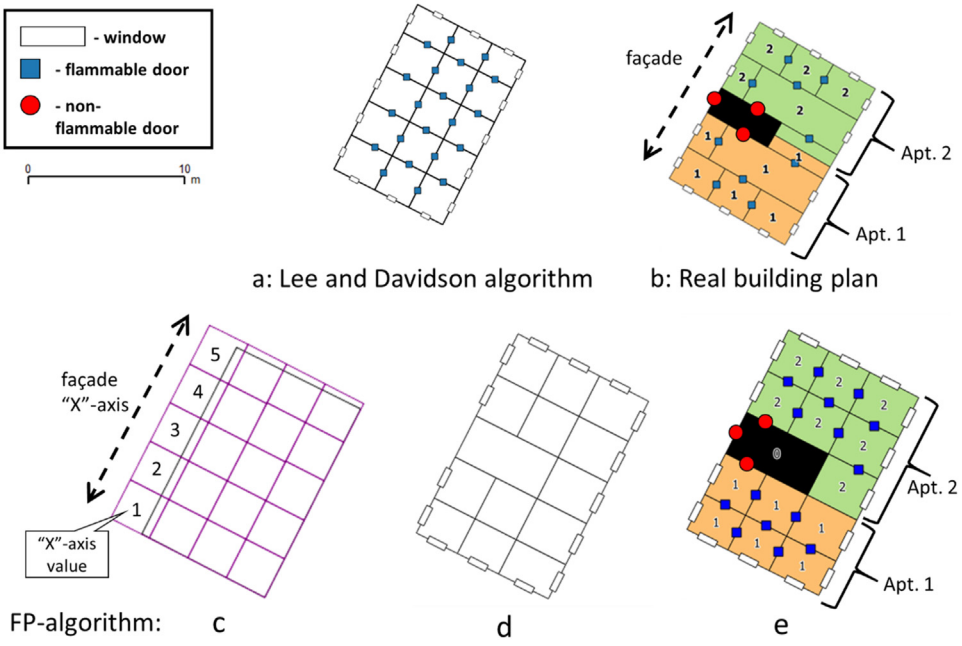

Fig. 3. Major steps of the FP-algorithm applied for partitioning of the building's ground floor in comparison to the building's plan and Lee and Davidson [1] partitioning algorithm: The outcome of the Lee and Davidson [1] algorithm (a); real plan of the ground floor (b); FP-algorithm: establishing minimal bounding rectangle and establishing room grid (c); FP-algorithm: merging small rooms and establishing internal corridor and windows in the outer wall (d); FP-algorithm: establishing fuel-empty corridor and apartments (final partition) (e).

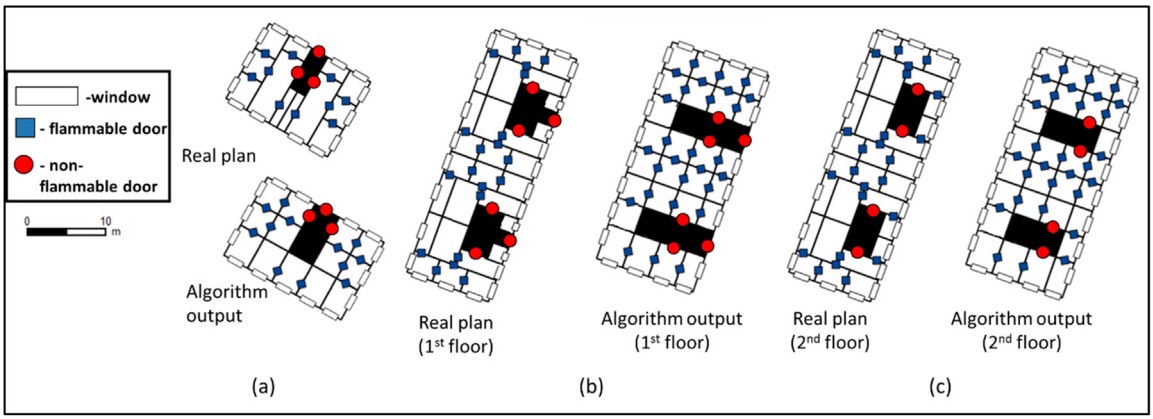

Fig. 4. Examples of the FP-algorithm output compared with real plans. One-floor building with one entrance (a); first floor of the building with two entrances (b); second floor for the building with two entrances (c).

apartment.

Fig. 4 presents three examples of the FP-algorithm and real plans. Examples (a-b) show the first floor of two buildings, with a single entrance (a) and two entrances (b). Example (c) shows the first and second floor of a building with two entrances.

2.4.3. Validation of partitioning algorithm sufficiency for modeling fire spread in non-flammable cities

To verify the sufficiency of the FP algorithm for modeling fire spread in non-flammable buildings, we compared the model outcomes for the Haifa residential neighborhood consisting of 105 residential buildings (Fig. 5) built in 1930's–1940's.

The spread of fire in the area was modeled for the time period of one hour, for the detailed plans of the buildings' interior with exact positions and sizes of windows and doors taken from the Haifa municipal archive [18] and two partition algorithms (1) FP-algorithm and (2) algorithm proposed by Lee and Davidson [1]. In the scenarios below, the ignition point was set in the south-east corner room of each building, the wind was set to west with speed of 4 m/s, and air temperature to 20 C [19]. Following [1], fuel load of occupied rooms was set to 16 kg/m^2 and fuel load of the corridors was set to zero. In what follows we compare the model fit for a randomly selected typical building and average model fit over all 105 buildings of the neighborhood. For three partitions we compare, as in [1,3], the dynamics of the total burnt area in the building.

Typical single building: The detailed floor plan of the typical building that was chosen for validation (Fig. 5c) is presented in Fig. 3.

Fig. 6 presents the total burnt area for each partition of this building. As can be seen, fire dynamics is almost identical for the partition obtained with the FP-algorithm and real building plan, while they are critically different for the partition proposed in [1].

Table 2
Average burnt area and the number of the burnt rooms in each building after 60 min of fire for two algorithms of building foundation partition into rooms and apartments.

	Real building plans [18]	FP-algorithm	Lee and Davidson algorithm [1]
Average burnt area, SE (m^2)	151.7 (4.9)	158.1 (6.6)	457.6 (31.8)
Average burnt rooms, SE	10.7 (0.3)	10.7 (0.4)	36.5 (2.6)

Neighborhood's average: According to the construction plans, 105 buildings in the area consist of 691 apartments and 5224 rooms of total floor area of 70525 m^2. The average burnt area and the average number of burnt rooms in each building after 60 min of fire for three partitions are presented in Table 2.

To conclude, despite some differences between the partitions obtained with the FP- algorithm and the real plan, the fire spread dynamics in these two cases is almost identical. For our model experiments below we exploit standard GIS layer of buildings represented by footprints and characterized by their height. To apply the model we consider each building as consisting of floors of 2.8 m height and then apply the FP-algorithm to partition each floor into apartments, rooms and corridors.

2.5. Building-to-building fire spread

During an urban fire, a building can be either ignited from the nearby building or from the burning vegetation. As discussed in Section 2.4.1, in both cases the ignition can be caused by impinging flames, by radiation or by brands - flying pieces of burning material. The model

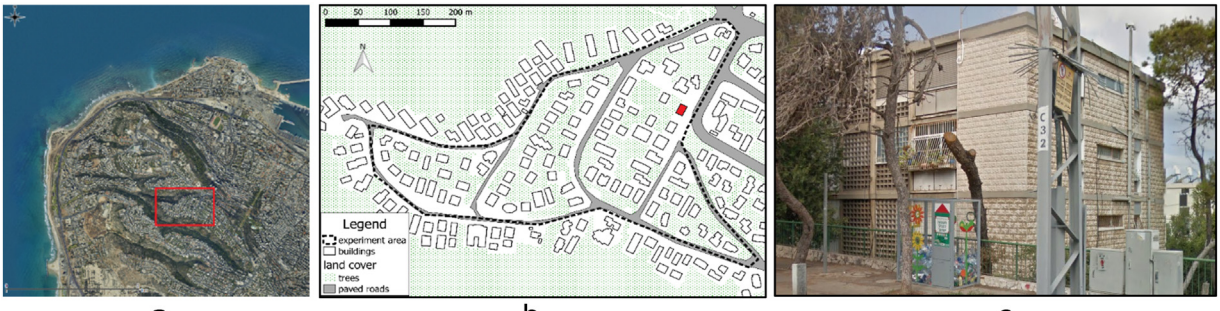

Fig. 5. Haifa residential neighborhood exploited for model/partitioning algorithm validation (a); close view of the neighborhood (b); a Google Street View of the typical buildings there marked red in the map (c).

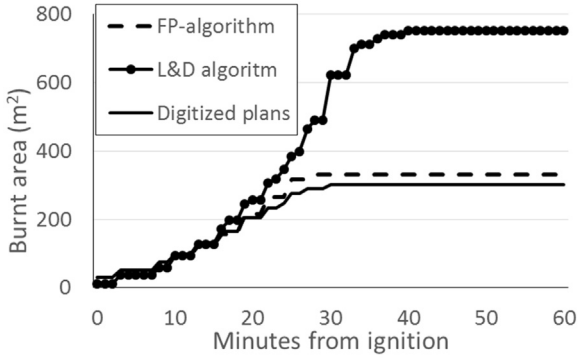

Fig. 6. Fire development in a typical Haifa building for different floor partitions: the real building plan, the Lee and Davidson's algorithm and the FP algorithm. Partitions' detailed are showed in Fig. 3.

should also include description of the fire spread within the vegetation.

2.5.1. Ignition of buildings by radiation from neighboring buildings

Following [1], we consider impinging flames, hot gas within rooms, and flames rising from burning flammable roofs as radiators. Since buildings' walls are non-flammable, only windows and flammable roofs in the line-of-sight from the radiator are considered as receivers. The geometry of flame is defined by the form of the windows and fire temperature inside the room, following [13,15], see Annex A.

Received radiation is calculated using Boltzmann equations (See Annex A). The visibility that defines the portion of received radiation is calculated based on the receiver's relative position to the radiator, as described in [16] (also known as 'configuration factor'). GAMA modeling software [11] provides a set of effective 3D spatial operators for these calculations.

When total radiation flux received by a window of a nearby building reaches a threshold level, in-room fuel is ignited. Flammable roofs are also ignited when the total received radiation reaches the same thresholds. Ignition time is inversely proportional to the flux and we employ the estimates proposed by [1]: for the steady radiation influx greater than 30, 20, 17.5, 15, or 12.5 kW/m^2, ignition of in-room fuel or target roof occurs after at most 1, 7, 10, 25, or 30 min, respectively.

2.5.2. Ignition of buildings by brands from neighboring buildings

Following Lee and Davidson [1], we assume the burning roofs create fire brands, i.e., small pieces of burning material flying downwind. Creation of brands is calculated based on Waterman's [20] experiments as a function of roof area and wind speed, as adopted in [1]. Brands' landing location is calculated according to Himoto and Tanaka [2]. When a brand lands on a roof, the probability that it will ignite the roof it lands on is set following [20] and is 1.75×10^{-3}.

2.5.3. Ignition of vegetation by flames from neighboring buildings

We assume that vegetation can be ignited by flames impinging from the windows or by brands from burning roofs. We assume that in the dry conditions of MME cities the impinging flames that touch the vegetation immediately ignite it.

2.5.4. Ignition of vegetation by brands from the neighboring building

Similar to Li and Davidson [10] we assume that vegetation cover is not continuous, even within the limits of the GIS layer of vegetated space. Therefore, ignition probability of vegetated space is linearly proportional to the vegetation cover density at a fine scale. For example, if only half of the surface within the layer is actually covered by vegetation, the probability of ignition is estimated as half of the basic ignition probability [20], that is, $1.75 \times 10^{-3}/2 = 0.875 \times 10^{-3}$.

2.5.5. Fire spread in vegetation

To the best of our knowledge, the dynamics of the fire spread in vegetation has been investigated and modeled for wildfires only. Wildfire dynamics in these models is based on a three-dimensional distribution of fuel at the scale of dozens of meters, see the frequently used models of [21,22] for notable examples. Such modeling approach is insufficient for modeling urban vegetation fires since fuel characteristics in the city essentially vary at a meter scale. As a result, modeling fire spread within urban vegetation is still in its initial stages, see [23] for a recent review.

To describe fire dynamics within urban vegetation we thus employ a simplified heuristic model that is based on the fuel-model for the relevant

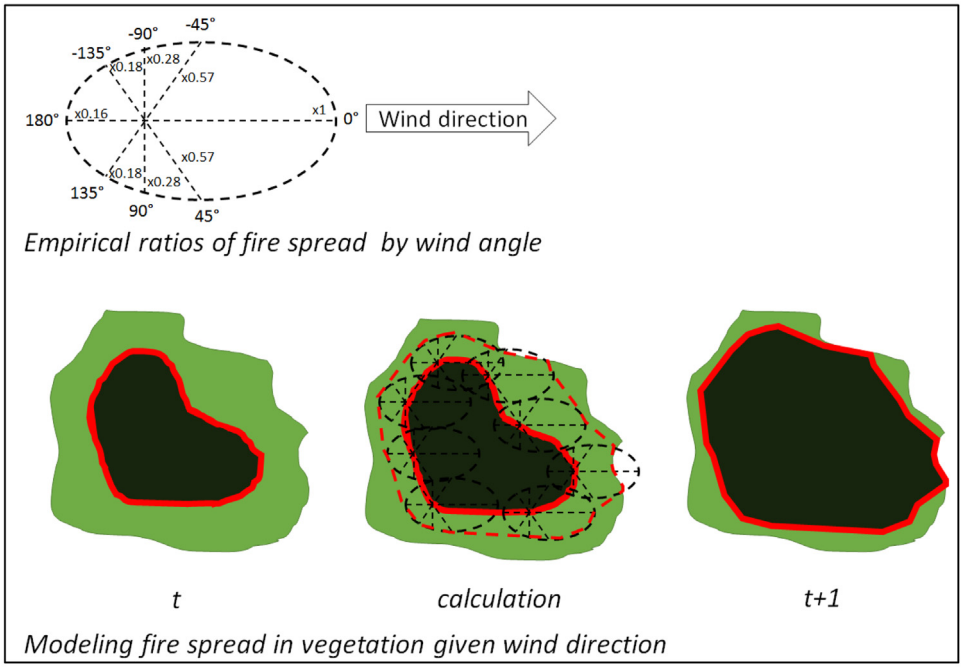

Fig. 7. Modeling fire spread in vegetation during a simulation tick (t→t + 1): Top - ellipse of fire spread according to [26]. Bottom - fire front spread during a model tick for West wind.

vegetation type (like timber, shrubs or grass) [24], accounting for the wind speed and fuel moisture. To account for the effect of wind direction we apply the ellipse of fire spread that represents the area of a fire spread from the point ignition during short time period proposed in [25].

According to this model, the area of a fire spread is an ellipse oriented towards wind direction, and the distance between one of the foci and the farthest point of the ellipse equals to the maximal distance of fire spread during simulation tick [25]. We have applied this model with the help of GAMA's [11] spatial library according to the following steps (Fig. 7): (1) Create points along the contour of the fire polygon at a tick t at distance of 1 m from each other. (2) Locate ellipses of fire spread at these points fitting ellipse's focus representing the basis of the wind vector (top of Fig. 7) to a point. (3) Build a convex hull of all the ellipses. (4) Intersect the polygon bounded by the convex hull with the polygon of the vegetation. The boundary of resulting polygon is the fire boundary at a tick $t + 1$. Note, that this approach can be extended for accounting the effect of slope on fire spread in vegetation [21,25].

2.5.6. Ignition of buildings by direct contact with vegetation

We assume that direct contact happens when the distance between the burning vegetation and windows is 0.5 m or less, due to flames tilting. We also assume that the flames of burning vegetation immediately lead to the ignition of touched room through the window.

2.5.7. Ignition of buildings by radiation from vegetation

The total radiation received by each window from vegetation is dependent on the vegetation type, the distance between burning vegetation and the window, and "burning time" – the length of the period during which the vegetation at this distance is burning (maximum 2 min) [27]. For the geographical regions that we consider (MME and similar) we distinguish three types of vegetation: shrubs, trees with short horizontal façade (5 m) characteristic of the urban area, and trees with long horizontal façade (10 m) characteristic of the rural area, as suggested by [27]. We assume that all radiation is absorbed by the receiver, since in NF-cities the vegetation surrounding the building and its façade straightly faces the windows.

Table 3 is adopted from [27] and gives the minimal time for igniting of target windows by constant radiation flux from vegetation in each range. For example, burning shrubs located 3 m from the window will ignite it if they are burning for 300 s, while trees with short horizontal façade will ignite it if they are burning for 60 s.

3. Case study: building fire risk maps for Haifa residential neighbourhood

3.1. Study area

We study fire spread patterns over a larger study area, a Haifa neighborhood of 452 buildings with 7418 apartments (total floor area 316,204 m^2) (Fig. 8). GIS layer of building footprints and heights was supplied by Survey of Israel and the FP- algorithm was applied to establish the internal structure of the buildings. Note that manual digitizing of the internal structure of building in the area would have taken several weeks.

Table 3
Minimal burning time (seconds) necessary for radiation ignition through window, by vegetation type and distance.

Distance to target window (m)	Shrubs	Trees, short façade	Trees, long façade
3	300	< 60	< 60
4	–	< 60	< 60
5	–	60	< 60
6	–	120	< 60
7	–	180	< 60
8–11	–	–	< 60
12	–	–	60
13	–	–	120
14	–	–	180
15	–	–	300

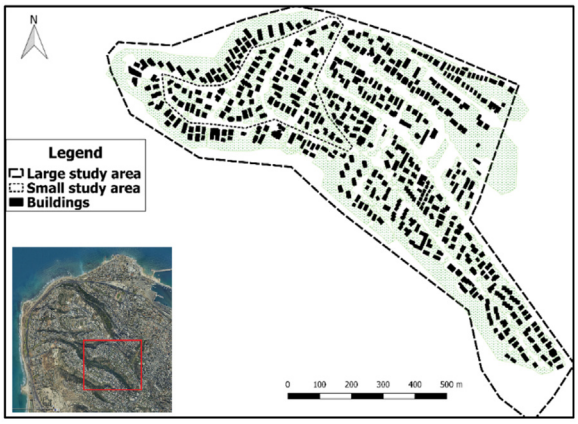

Fig. 8. Larger case study area in Haifa, Israel. Smaller initial study area which was used to validate the FP- algorithm is marked by the dashed line.

Table 4 shows the distribution of wind conditions as measured by the Israeli Meteorological Service in the Haifa University measurement station, the nearest to the study area [19].

The common winds are west and north winds, arriving from the Mediterranean Sea. In this section, we focus on creating risk maps for these winds, yet the same procedure may be used to create risk maps for all wind conditions.

We ran the model for the common west and north winds at speeds of 4, 6 and 8 m/s. West winds at those speeds occur in frequencies of 11%, 8%, 4%, while north at the frequencies of 6%, 3%, and 1% respectively.

3.2. Simulation procedure and parameters

To systematically study risk across the study area and with respect to different meteorological conditions, we focused on fires starting in ground floor apartments in each one of the buildings. Fires that start at the ground floor apartments are maximally risky for the entire building, since fire spreads upwards and since vegetation is attached to the ground. For each meteorological condition we have conducted 1614 runs, according to the number of ground floor apartments in the study area.

In each run, a different ground-floor apartment was chosen and one of its rooms was randomly ignited. We named this apartment as "origin apartment". Each model experiment was run for 60 min at a temporal resolution (simulation 'tick') of one minute.

We used high-resolution aerial photos (0.5 m/pixel) to digitize a GIS layer of vegetation. We calculated fire spread in the vegetation using the selected fuel model ("Moderate Load Dry Climate Shrub" - SH2/142, [24]) for two moisture levels: "moderate" representing spring, and "dry" representing summer or autumn. We also applied the correction of [28] and factored speed down by 2 for this vegetation type in this area. Maximal speed of downwind fire spread in vegetation for the studied wind speed of 4, 6 and 8 m/s respectively are 0.011, 0.019, 0.027 m/s for the moderate moisture conditions, and 0.016, 0.027, 0.052 for the dry conditions, respectively.

As explained in Section 2.5.4., the probability of vegetation ignition by brands released from burning roofs is defined by the fraction of the ground that the vegetation covers within the layer boundaries. Based on the aerial photos, this fraction is about 0.25 and we thus set the probability of ignition equal to 0.25 times probability of brands to ignite roofs. Numerically, this probability is set to 4.375×10^{-4} for each fire brand landing inside the GIS vegetation layer. Air temperature is set equal to 20C, typical for the near meteorological station [19].

Table 4
Wind distribution at Haifa University meteorological station 2006–2011 [19].

Dir	< 1 m/s	1–2 m/s	2–4 m/s	4–6 m/s	6–8 m/s	8–10 m/s	10–12 m/s	12–14 m/s	14–16 m/s	Total
N	0%	5%	6%	3%	1%	0.2%	0%	0%	0%	**15%**
NE	0%	2%	3%	2%	1%	0.2%	0.1%	0%	0%	**8%**
E	0%	2%	3%	3%	3%	1.3%	0.7%	0.3%	0.1%	**13%**
SE	0%	0%	1%	0%	0%	0.1%	0%	0%	0%	**2%**
S	0%	1%	1%	1%	0%	0%	0%	0%	0%	**2%**
SW	0%	2%	5%	7%	5%	2.3%	0.9%	0.4%	0.1%	**23%**
W	0%	5%	11%	8%	4%	1.3%	0.3%	0.1%	0%	**29%**
NW	0%	5%	2%	0%	0%	0%	0%	0%	0%	**7%**
Tot	**1%**	**22%**	**30%**	**24%**	**14%**	**5%**	**2%**	**1%**	**0%**	**100%**

4. Results

The following results clearly demonstrate that burning vegetation is almost the sole mechanism for fire spread between buildings in the study area and that the effect of wind on the speed of the fire spread in essentially non-linear. The relative spatial distribution of risk is determined by the properties of the building and its close surroundings.

4.1. Relative importance of the factors of fire spread

As presented in Section 2 we distinguish between four fire spread mechanisms: R-radiation, D-direct ignition, B-brands, V-vegetation. For each fire we have recorded the mechanisms that were responsible for fire spread and Table 5 presents the frequencies of various subsets of these four mechanisms observed in simulations, for different wind speeds. If the fire had spread to the neighboring buildings, the efforts needed to extinguish it significantly increase. That is why, for each wind speed and combination of fire-spread mechanisms, we also present the average, per ignition, number of buildings to which the fire had spread and the STD of this number.

Table 5 shows that the share of simulation runs in which fire spread only by direct contact has a share of one third, and that these cases are limited to building of origin. In the rest two thirds (62–64%) of cases, fire spreads mostly following ignition of the inter-building vegetation. This share of cases is almost independent of the wind speed. These two finding are a consequence of the relatively large gaps between buildings in the study area (m = 7 m, STD = 3.2 m) - in two third of cases this gap is larger than the effective range of radiation or direct contact.

Note that, with the increase in wind speed, fire spread in vegetation is more and more oriented downwind and the chance that only the buildings in direct downwind location will be ignited increases. For example, for the case of north (180°) wind at 6 m/s the average difference between the wind direction and the direction between the building of origin and the next ignited building is 0.3° and in 68% of the cases it is less than 45° (STD = 55.2°).

An unintended confirmation of the importance of the urban fire spread through vegetation has been the breakout of a large fire in Haifa, Israel in November 2016, less than 3 km south of our study area. The extreme meteorological conditions made it very difficult to extinguish the fire which, according to reports in media, mostly spread through vegetation and brands [29] and destroyed more than 500 residential apartments. According to other media reports, the lack of vegetation management was a major reason for these severe results [30].

4.2. Mapping risk over the study area

The fraction of simulation runs in which vegetation in a study area is ignited always remains at a level of 62–64% (Table 5). This suggests that the factors which lead to vegetation ignition are related to the properties of the building and its close surroundings. To verify, we created maps of potential fire spread for the different wind conditions (Fig. 9). Each map shows the average number of buildings to fire had spread by building of origin and wind conditions. These maps show that even though the overall risk changes with wind conditions, the same areas remain dangerous ones under all wind conditions.

The zoom windows in Fig. 10 show that the distance to the vegetation is critical for the fire spread. In case the vegetation is relatively far (Fig. 10a) the risk of the fire spread is low, in case it is close (Fig. 10b) the risk is high. Such maps and origin-to-target calculation can help firefighters and other authorities to plan fire mitigation and response.

4.3. Simulating mitigation policies

The identification of risk factors controlling fire spread may be used to design policies for risk reduction. Since fire spread through vegetation is the major fire spread mechanism in MME cities, we studied two potential policies: (1) cutting vegetation branches over paved roads, and (2) cutting vegetation in 4 m range around buildings. We used the aerial photos to identify paved roads, and standard GIS functions to create three new vegetation layers: the first two layers represent the implementation of each policy separately, and the third represents the implementation of both policies.

The motivation for analyzing the two policies emerges from the major role that urban vegetation holds for MME cities in the general context. As mentioned in the introduction, MME cities are characterized by hot, long and dry summers, which lead to planting dense vegetation within the city. Aside for its aesthetic function therefore, such vegetation acts as a cooling and shading urban component. This leads many urban residents to oppose to the reduction of vegetation, despite its risks in fire scenarios. The first policy, that of cutting vegetation over paved roads, can be carried out by local authorities without requiring

Table 5
Percentages of fire spread mechanisms in simulation runs, and average (STD) of the number of ignited building for each mechanism.

Wind speed	4 m/s		6 m/s		8 m/s	
	Percentage of occurrence	Average and STD of the number of ignited buildings	Percentage of occurrence	Average and STD of the number of ignited buildings	Percentage of occurrence	Average and STD of the number of ignited buildings
D	38%	–	36%	–	36%	–
D + B	2%	0.01 (0.11)	1%	0.02 (0.15)	1%	0.04 (0.19)
D + V	50%	0.46 (0.86)	50%	0.96 (1.34)	52%	0.67 (1.2)
D + V + B	10%	0.75 (0.89)	13%	1.38 (1.22)	11%	1.20 (1.21)

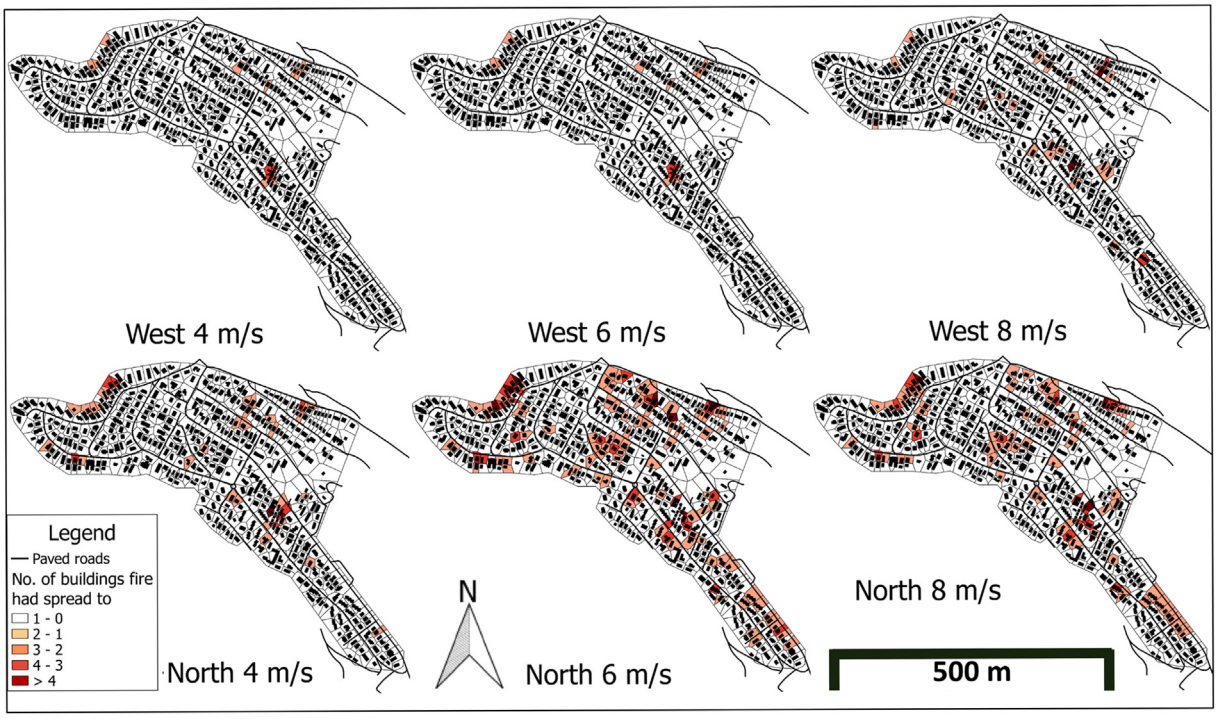

Fig. 9. Risk maps of the average number of buildings a non-extinguished fire had spread to within 1 h, by building of origin and wind conditions.

residents' approval. The second policy, cutting vegetation around each building, may demand residents' approval and is more likely to encounter opposition. In addition, the first policy is expected to demand less financial resources.

We simulated the policies' effects conducting three sets of simulation runs: one for each vegetation layer: (1) cut over roads, (2) cut in 4 m range around buildings, and (3) cut over roads and in 4 m range around buildings. We conducted each set of runs in the manner described at the previous section: running the model 1614 runs while igniting a different ground floor apartment in each run. We used the

Table 6
Policy analysis.

Policy	Burnt floor area (m^2) average (STD)	Total ignited buildings average (STD)
base case	369.32 (318.13)	0.47 (0.85)
cut over roads	370.25 (321.51)	0.47 (0.83)
cut around buildings	139.02 (129.55)	–
cut over roads + around buildings	136.98 (130.72)	–

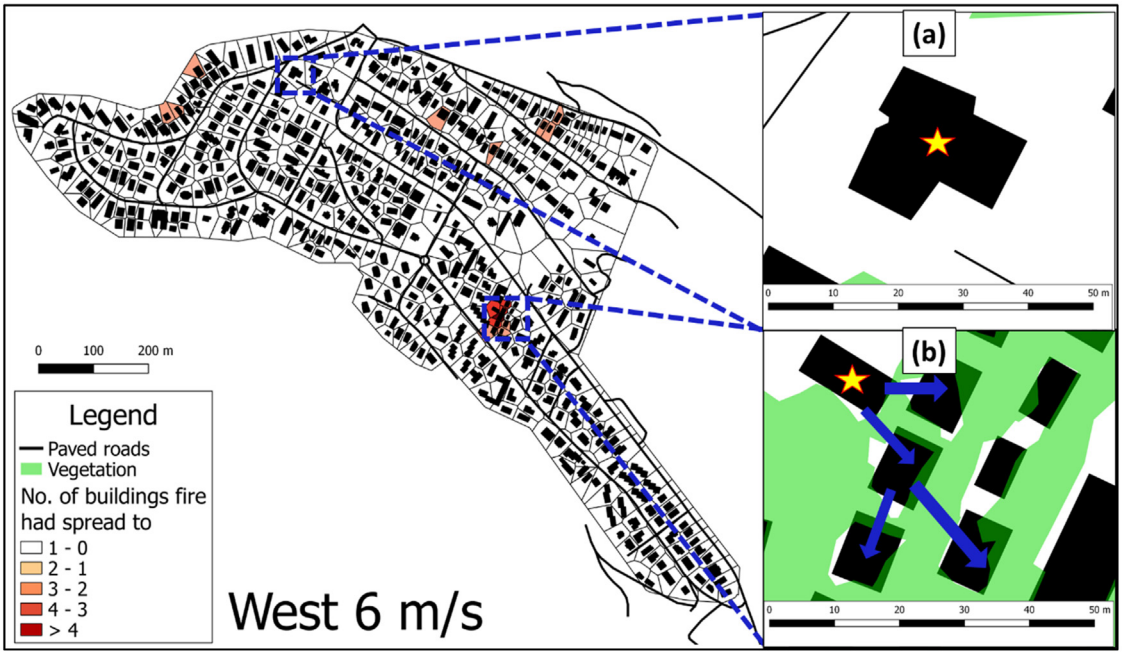

Fig. 10. (Left) the average number of buildings a non-extinguished fire had spread to within 1 h for 6 m/s north wind, by building of origin; (a) fire spread around low-risk location; (b) fire spread in 1 h around the most risky location.

case of west wind of 6 m/s and moderate vegetation moisture. All other experimental parameters were identical to those used in Section 3.

Table 6 gives the results of all three policies application. *'Burnt floor area'* stands for the total floor area of ignited rooms, and *'ignited buildings'* stands for number of additional buildings fire had spread to.

Cutting vegetation around buildings has a strong effect of reducing fire spread, almost 3 times compared to the base case. Cutting vegetation over roads does not have any significant effect.

We conclude that policies of vegetation management carry a major potential for reducing fire spread in MME cities. Cutting trees around all building may be a too drastic measure. Detailed policies may be designed by assessing the fire risk of each building separately and cutting vegetation around the more dangerous ones.

5. Discussion and conclusions

We introduced, validated, and investigated a city-scale model for fire spread in cities of non-flammable buildings, in which the space between buildings is partially filled with highly flammable vegetation. The model of fire spread within the building is based on the novel algorithm for generating intra-building partitioning into rooms, apartments and corridors. We demonstrate that the obtained partition, even if different from the real one, is sufficient for adequate representation of the fire spread in non-flammable buildings. In this way, we became able to exploit a standard GIS layer of building footprints for modeling urban fire spread at the city-scale.

Fire spread between buildings is defined by the pattern of urban vegetation, and ignition of vegetation is responsible for more than 60% of the cases of fire transmission from building-to-building. Vegetation pattern is thus a major factor of fire spread in cities of non-flammable buildings. This is basically different from cities of flammable buildings, where a major factor of the fire spread is radiation from burning buildings. Even in the forest-situated Grass Valley, CA community where all buildings are flammable, only 30% of the buildings were ignited by burning vegetation [10].

In case the vegetation pattern is dense, the importance of other factors becomes essentially low and we demonstrated this phenomenon for the case of the Israeli city of Haifa, where the variation in meteorological conditions does not significantly influence the spatial distribution of relative fire spread risk. The spatial precision of the vegetation pattern becomes thus critical for successful use of the model.

Our model allows to identify urban locations and neighborhoods where the consequences of fire will be most dangerous, and to construct the risk maps. These maps clearly point to the neighborhoods and building for which risk of fires can be essentially reduced by proper managing of the vegetation in the buildings' proximity.

The maps of the fire spread risks are especially important in case of multiple ignitions that become highly probable after earthquakes or large forest fires at the city boundary. High spatiotemporal variation in the fire spread conditions and essential stochastic component in fire dynamics can turn these fires into primary urban disaster [1,2]. In these circumstances, firefighters should decide, in real-time, which fires to attend to. The maps of the risk of fire spread are critical for such prioritizing.

In this paper, we present the basic version of a model that should be yet elaborated in several respects. First, it should account for the city 3D structure represented by a digital elevation model (DEM). Second, the building partition should be further enhanced by accounting for the built elements that are important for the fire spread, such as elevator shafts or staircases. An experimental fire study may also improve the model predictions; however such experiments are expensive and to best of our knowledge can be performed only in a limited number of countries. Last, but not least, the model of fire spread in urban vegetation is only a first approximation of reality and, as mentioned in [23], should be critically improved and essentially better evaluated.

The model of fire spread in cities of non-flammable buildings is the basis for developing firefighters' decision support system. To complete such a system, we need to couple it with the model of firefighters' reaction and decision-making that is now in development. Our next step is to couple these two models to establish an agent based model and a serious game system for supporting firefighters' preparedness to multiple-ignitions in the Mediterranean and Middle Eastern cities of high danger of seismic activity (see [31]).

Acknowledgements

We would like to thank Dr. Zoe Gutzeit for her proofreading. We would like to thank Yulia Grinblat (Porter School of Environmental Studies, Department of Geography and Human Environment, Tel Aviv University, Tel Aviv, Israel) and Dr. Marina Toger (ComplexCity research lab, Faculty of Architecture and Town Planning, Technion—Israel Institute of Technology, Haifa, Israel) for their agreement to use their aerial photos.

This paper is a result of a PhD study conducted at the Porter School of Environmental Studies, Tel Aviv University. Yonatan Shaham is supported by the Smaller-Winnikow Foundation and the Porter School of Environmental Studies, Tel Aviv University.

Appendix A. : MME fire spread model equations

Equations of parametric fire development model

According to Law, O'Brien [13]:
Abbreviations:

- $\dot{m}_r$ – rate of burning (kg/s)
- A_d – windows area (m^2)
- h_d – window height (m)
- d_r – room depth (m)
- w_r – rooms width (m)
- T_r – room temperature during the fully-developed fire phase (K)
- T_a – ambience temperature (K)
- $A_{r,F}$ – floor area (m^2)
- $A_{r,T}$ – total area of floor, ceiling, and walls minus total window area (m^2)
- L – total room fire load (kg)
- L" – occupancy-dependent fire load density (kg/m2)
- L_t – the percentage of fire load burned at time t

In room fire development for non-draft conditions (Eq. (2) is modified as described in Section 2.3):

Rooms with one window: $\dot{m}_r = 0.18(1 - e^{-0.036\eta})A_d\,(h_d{}^{0.5})\left(\frac{d_r}{w_r}\right)^{0.5}$ (1)

*Rooms with two windows: $\dot{m}_r = 1.7 \times 0.18(1 - e^{-0.036\eta})A_d\,(h_d{}^{0.5})\left(\frac{d_r}{w_r}\right)^{0.5}$ (2)

$T_r = T_a + 6000(1-e^{-0.1\eta})(1-e^{-0.05\psi})\eta^{0.5}$ (3)

$\eta = \frac{A_{r,T}}{A_d h_d{}^{0.5}}$ (4)

In room fire development for draft conditions:

$\dot{m}_r = \frac{L}{1200}$ (5)

$T_r = T_a + 1200(1-e^{-0.04\psi})$ (6)

General equations:

$L = A_{r,T}L'$ (7)

$\psi = \frac{L}{\sqrt{A_d A_{r,F}}}$ (8)

$L_t = \frac{\dot{m}_r}{L}$ (9)

When: $0.3 \le L_t \le 0.8$ – fire is in the fully − developed phase (10)

Equations for geometry of flame impinging from windows

Based on experiments of Law and O'Brien [13] and Klopovic and Turan [15]
Abbreviations:

- w_w – flame width (m)
- h_w – height of the flame tip above the top of the window (m)
- w_d – window width (m)
- λ_w – flame thickness (m)
- x_w – projection of the centerline of the flame (m)
- u – wind speed (m/s)

For non-draft conditions:

$h_w = 12.8\left(\frac{\dot{m}_r}{w_w}\right) - h_d$ (11)

$w_w = w_d$ (12)

$\lambda_w = \frac{2h_d}{3}$ (13)

$$\begin{cases} x_w = \frac{h_d}{3} \text{ If there is a wall above the window and } h_d < 1.25w_d \\ x_w = 0.3h_d\left(\frac{h_d}{w_w}\right)^{0.54} \text{ If there is a wall above the window and } h_d \ge 1.25w_d \\ x_w = 0.6h_d\left(\frac{h_w}{h_d}\right)^{\frac{1}{3}} \text{ If there is no wall above the window} \end{cases}$$ (14)

For through-draft conditions downwind window only:

$h_w = 23.9u^{-0.43}\dot{m}_r A_d{}^{-0.5}$ (15)

$\lambda_w = h_d$ (16)

$x_w = 0.605(\frac{u^2}{h_d})(h_w + h_d)$ (17)

Radiation equations

Abbreviations:

- ϕ – configuration factor

- ε – emissivity
- σ – Stefan-Boltzmann constant: 5.67×10^{-12} W/m^{2}K^4
- T – temperature of radiator (K)
- T_a – ambient temperature (K)

Equation:

Boltzmann equation for absorbed radiation: $q'' = \phi\varepsilon\sigma(T^4 - T_a^4)$ (18)

For gas: $\varepsilon = 1$ (19)

For window flames: $\varepsilon = 1 - e^{-0.3\lambda_w}$ (20)

Appendix B. : Footprint Partitioning (FP) algorithm

The FP-algorithm for partitioning of the building footprint into rooms, apartments and corridors aims at substituting Lee's algorithm of partitioning building footprint into rooms [16]. It is designed for residential buildings of unlimited length and of the width of up to 70 m and implemented with GAMA [11]. The GAMA software for the PF-algorithm is freely available at https://github.com/YonatanShaham/MME_fire Parameter values used in this article are given in (Table B1).

Table B1
Algorithm parameters and values used in this article.

Algorithm parameter	The value used in this paper
Typical floor area of apartment (A)	80 m^2 (Haifa municipal archive)
Dimensions of a typical square room (RxR)	3.5 × 3.5 m = 12.25 m^2 (Haifa municipal archive)
Minimal room area (m)	7 m^2 [16]
Minimal length of a wall with a window (W)	2 m (Haifa municipal archive)
Create internal corridors above ground floor? (Yes/No)	Yes
Fuel load in rooms (L)	16 kg/m^2 wood equivalent [1]

1. **Build Rectangle of Minimal Area (RMA) containing building's footprint**

– –Build convex hull of the footprint
– Loop by hull edges
  – If hull's edge is the edge of the footprint build minimal bounding rectangle (MBR) with a side containing an edge
– Select MBR of the minimal area Fig. B1

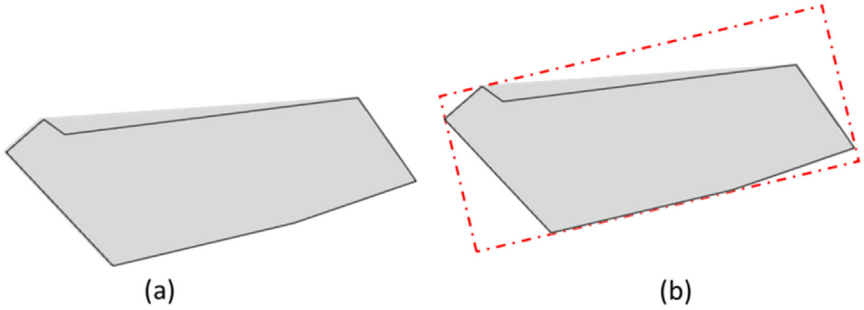

Fig. B1. Convex hull of a building footprint (a); Minimal bounding rectangle of the minimal area (b).

– Set the long side that is closer to the nearest road as building's “facade”.
– Cover MBR by a grid of RxR cells, starting from the left bottom corner. Denote number of cells along the facade as l and along the short side of the MBR as s.
– If $l > 5$ divide the grid along the facade into entrance sections - grid blocks of a 5-cell width (Fig. B2).
– If the width of residual entrance is 2 or less – include it to the previous one. Otherwise make it a separate entrance.

– Process each entrance depending on s
– If $s \leq 6$ do nothing
– If $7 < s \leq 10$ divide each entrance section into two, of height 5 and $s - 5$
– If $10 < s \leq 14$ divide each section into two, one of the height INT(s/2), and one of s – INT(s/2)
– If $s > 14$ (building width exceeds 70 m) report “error, width of the building exceeds 70 m)
– If the section dimensions are 3 × 3, 3 × 4, or 4 × 4 cells apply special rules (Special cases section), else apply regular rules

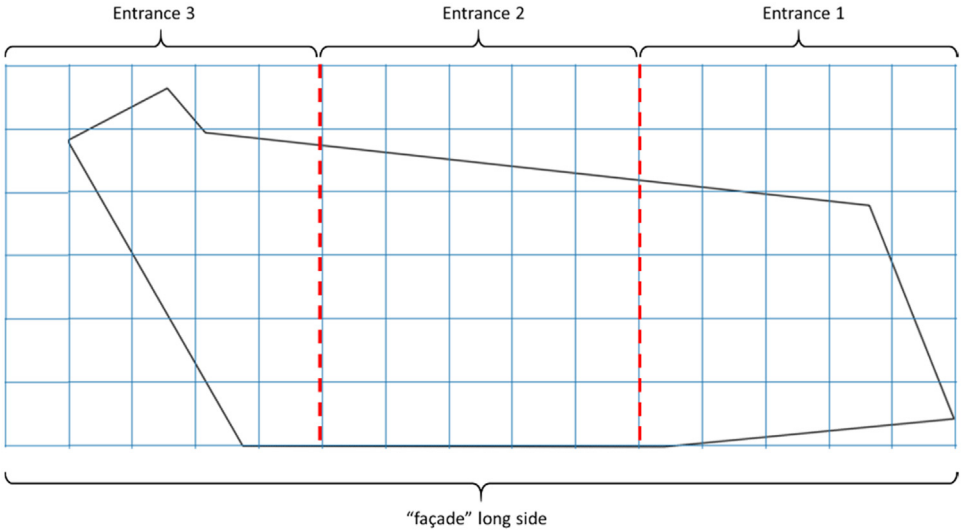

Fig. B2. Partition of an MBR into entrances.

2. **Build rooms**

– Overlap cell grid and the footprint polygon
– Consider each polygon of the overlap. Merge polygons of an area less than m with the adjacent full cell and denote the resulting polygons as "rooms" (Fig. B3)

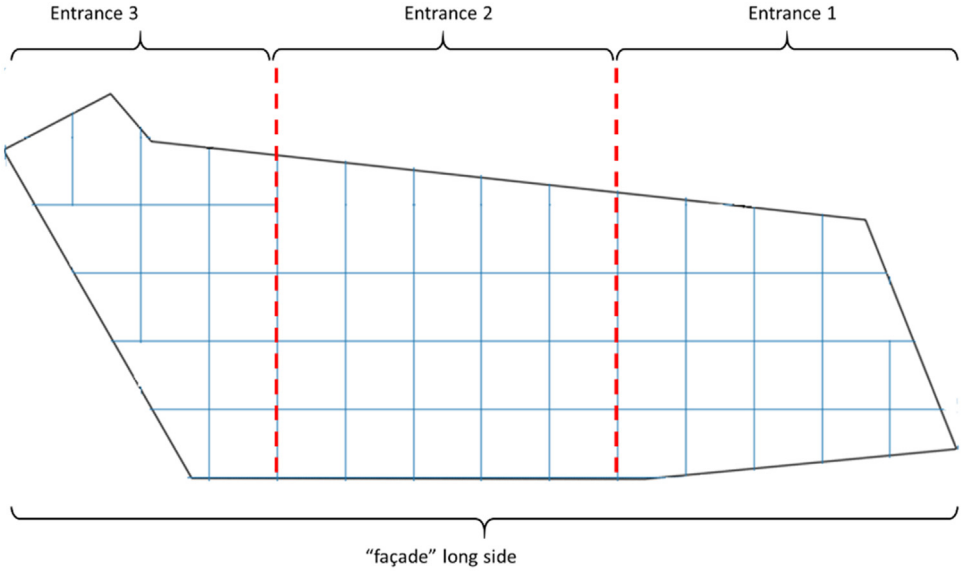

Fig. B3. Building rooms: merge partial cells and adjacent full cell.

3. **Build corridors**

For each entrance section:

– Establish *external* ring of rooms consisting of rooms one side of which belongs to the boundary of an entrance section. Establish *internal* rings of rooms as the set of cells adjacent to the external ring.
– Select the longest side of the entrance section that is also the footprint's edge. Select room in the middle of the row of rooms adjacent to this edge and set it as a corridor's entrance.
– Consider room of the internal ring that has a common edge with the corridor's entrance and merge it with a corridor's entrance. Continue merging rooms in the same direction, until another room of the external ring is reached again. Do not include this last room into a corridor (Fig. B4).

– If the parameter "Create internal corridors above ground floor" is "False", create corridors in floors above the ground floor in the same way as with the ground floor.
– Else, for floor above the ground floor, skip the room in the middle of the row (outer ring) and start merging rooms into a corridor from the room of the internal ring that has a common edge with the in the middle of the row (outer ring

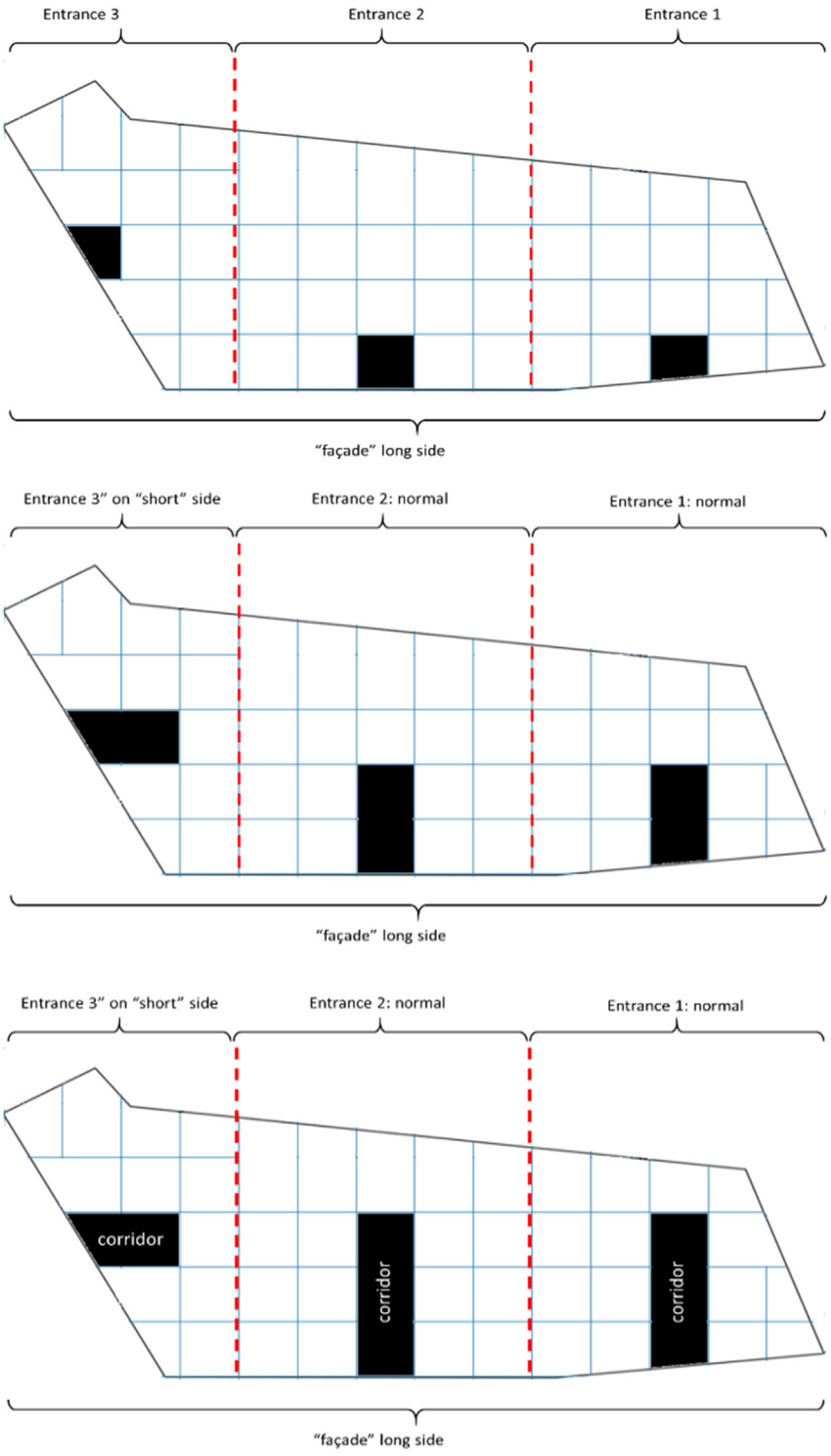

Fig. B4. Sequential steps of corridor construction.

4. **Accumulation of rooms into apartments**

- Start with the room of external ring at the left of the entrance, follow the external ring, and accumulate rooms to the external part of the first apartment until the total floor size of the accumulated rooms exceeds A/2 (half of the typical apartment floor area in the study area).
- Consider the room of external ring adjacent to the last of the rooms of the established external part of the apartment and accumulate rooms of the external ring to a new apartment until the total floor size of the accumulated rooms exceeds A/2.
- If the total floor area of the last set of external rooms is below A/2, then include them into a previous apartment Fig. B5

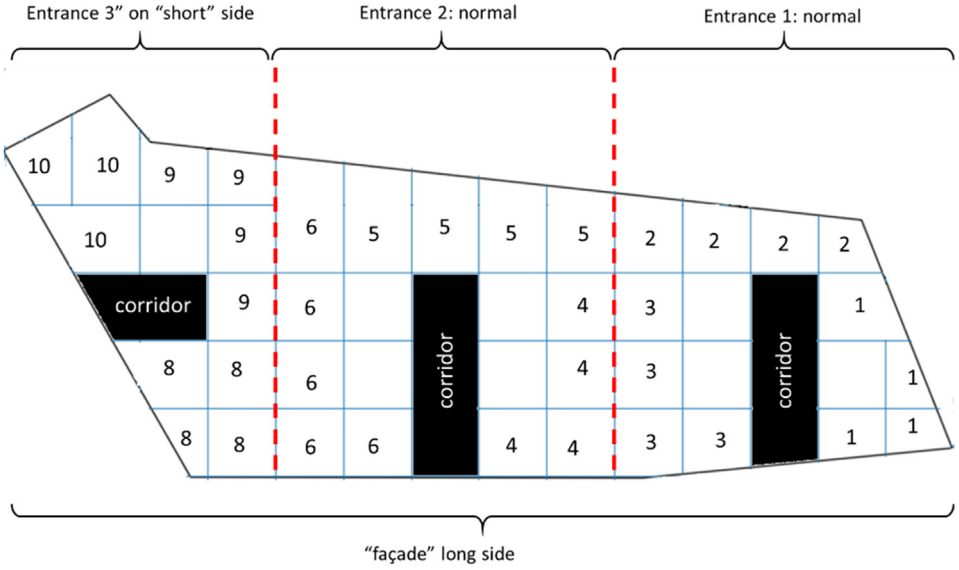

Fig. B5. Accumulation of external rooms into apartments.

– For each room of the internal ring consider apartments with the rooms adjacent to this room and estimate the length of the common boundary between this room and apartment's rooms. Join the room to the apartment with which this length is maximal. If this length is the same for two or more apartments, join the room to the apartment of minimal accumulated area. If minimal accumulated area is the same for more than one apartment choose one of them randomly (Fig. B6).

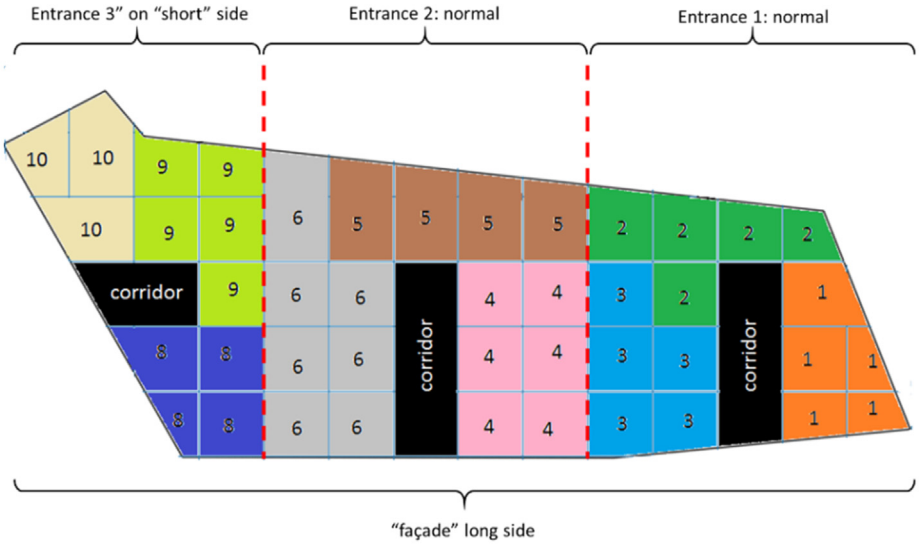

Fig. B6. Accumulation of internal rooms to apartments.

– If the resulting apartment has 1 or 2 rooms only, revoke it and join each of its rooms to adjacent apartments following general rules of accumulating rooms of the external and internal rings into apartments

5. **Establishing windows and doors**

– Loop by external walls of each room. Divide the wall into intervals of length *W*. If there is a residual interval add it to the previous one. Set a window in the middle of each interval
(Fig. B7)
– Loop by internal walls of each room. Establish a flammable door between each two rooms of the same apartment (Fig. B7)
– Consider apartment's rooms that have a common border with the corridor. Establish a non-flammable door to the corridor in the room that closest to the corridor's entrance (Fig. B7).

6. **Establishing fuel load**
   – Assign fuel load L to every room; assign zero fuel load to a corridor.
7. **Special cases** (both dimensions of a section are less than 5)

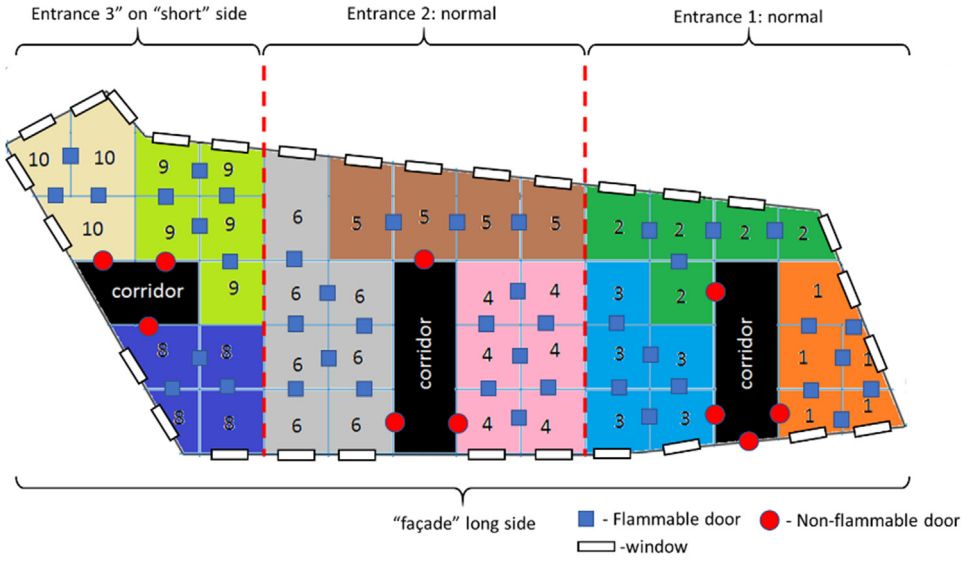

Fig. B7. Establishing windows and doors.

– Do not establish corridors.
– Establish apartments as in Fig. B8
– Establish windows and internal doors as in a general case
– Establish entrance doors as in Fig. B8.

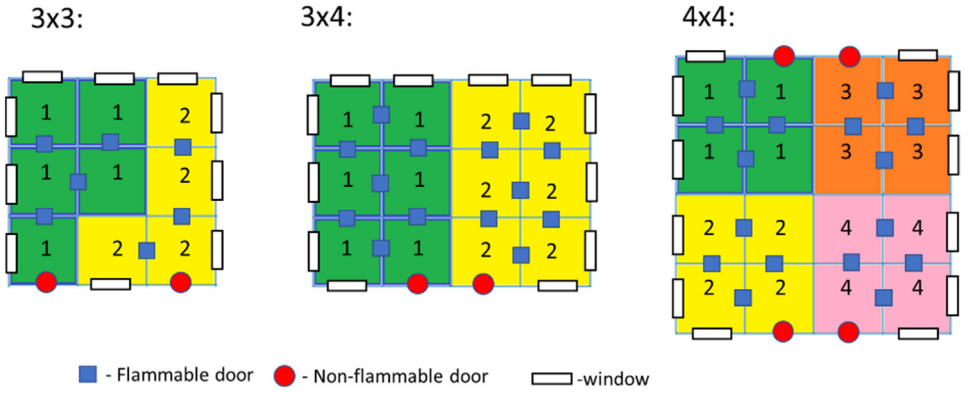

Fig. B8. Footprint partition in special cases.

References

[1] S.W. Lee, R.A. Davidson, Physics-based simulation model of post-earthquake fire spread, J. Earthq. Eng. (2010) 670–687.
[2] K. Himoto, T. Tanaka, Development and validation of a physics-based urban fire spread model, Fire Saf. J. no. 43 (2008) 477–497.
[3] S. Zhao, GisFFE—an integrated software system for the dynamic simulation of fires following an earthquake based on GIS, Fire Saf. J. no. 45 (2010) 83–97.
[4] G. Cox, S. Kumar, Modeling Enclosure Fires Using CFD, in: P.J. DiNenno (Ed.), SFPE Handbook of Fire Protection Engineering, National Fire Protection Association, Quincy, MA, 2002(pp. 3-194-3-218).
[5] N.D. Pope, C.G. Bailey, Quantitative comparison of FDS and parametric fire curves with post-flashover compartment fire test data, Fire Saf. J. (2006) 99–110.
[6] W.D. Walton, Zone computer fire models for enclosures, in: P.J. DiNenno (Ed.), SFPE Handbook of Fire Protection Engineering, National Fire Protection Association, Quincy, MA, 2002, pp. 3–190-3-193.
[7] F. Zhuman, G. Hadjisophocleous, A two-zone fie growth and smoke movement model for multi-compartment buildings, Fire Saf. J. 34 (2000) 257–285.
[8] C.R. Barnett, BFD curve: a new empirical model for fire compartment temperatures, Fire Saf. J. (2002) 437–463.
[9] J. Zehfuss, D. Hosser, A parametric natural fire model for the structural fire design of multi-storey buildings, Fire Saf. J. (2007) 115–126.
[10] S. Li, R.A. Davidson, Application of an urban fire simulation model, Earthquake Spectra 29 (4) (2013) 1369–1389.
[11] A. Grignard, P. Taillandier, B. Gaudou, D.-A. Vo, N.-Q. Huynh, A. Drogoul, GAMA 1.6: advancing the art of complex agent-based modeling and simulation (*vol.*), Lecture Notes Comput. Sci. 8291 (2013) 117–131.
[12] M. Law, Fire safety of external building elements–The design approach, Eng. J. 15 (1978) 59–74.
[13] M. Law, T. O'Brien, Fire and Steel Construction: Fire Safety of Bare External Structural Steel, Ascot: Constrado, 1981.
[14] T. Lennon, D. Moore, The natural fire safety concept—full-scale tests at Cardington, Fire Saf. J. 38 (2008) 623–643.
[15] S. Klopovic, O. Turan, A comprehensive study of externally venting flames —: part II: plume envelope and centre-line temperature comparisons, secondary fires, wind effects and smoke management system, Fire Saf. J. (2001) 135–172.
[16] S.W. Lee, Modelling post-earthquake fire spread (Ph.D. Dissertation), Cornell University, *I*thaca, NY, 2009.
[17] G. Proulx, Highrise Evacuation: a Questionable Concept, National Research Council, Canada, Boston, MA, 2001.
[18] Haifa Municipality, "Haifa Municipal Building File Archive (Hebrew)", 2009. [Online]. Available: ⟨http://147.236.237.215/haifa/tikim.htm⟩. (Accessed 17 4 2016).
[19] Israeli Meteorological Service, Wind Speed and Azimuth Records 2006–2011, Haifa University Station, Israeli Meteorological Service, 2012.
[20] T.E. Waterman, Experimental Study of Firebrand Generation, IIT Research Institute, Chicago, IL, 1969.
[21] R.C. Rothermel, A Mathematical Model for Predicting Fire Spread in Wildland Fuels, Forest Service, U.S. Department of Agriculture, Ogden, Utah, 1972.
[22] M.A. Finney, FARSITE: Fire Area Simulator-model development and evaluation, U.S. Department of Agriculture, Forest Service, Rocky Mountain Research Station,

Ogden, UT, 2004.
[23] S.L. Manzello, T. Yamada, A. Jeffers, Y. Ohmiya, K. Himoto, A.C. Fernandez-Pello, Summary of workshop for fire structure interaction and urban and wildland - urban interface (WUI) Fires –operation Tomodachi– fire research, Fire Saf. J. 59 (2013) 122–131.
[24] J.H. Scott, R.E. Burgan, Standard Fire Behavior Fuel Models: a Comprehensive Set for Use with Rothermel's Surface Fire Spread Model, U.S. Department of Agriculture, Forest Service, Rocky Mountain Research Station, Fort Collins, CO, 2005.
[25] D.R. Weise, G.S. Biging, Effects of wind velocity and slope on fire behavior (in), Fire Saf. Sci. (1994).
[26] F.A. Albini, Estimating Wildfire Behavior and Effects, U. S. Department of Agriculture, Ogden, Utah, 1976.
[27] J.D. Cohen, B.W. Butler, "Modeling Potential Structure Ignitions from Flame Radiation Exposure with Implications for Wildland/Urban Interface Fire Management", in: Proceedings of the 13th Fire and Forest Meteorology Conference, Lorne, Australia, 1996.
[28] Y. Carmel, S. Paz, F. Jahashan, M. Shoshany, Assessing fire risk using Monte Carlo simulations of fire spread, For. Ecol. Manag. 257 (2009) 370–377.
[29] BBC, "Israel fires: Tens of thousands flee as fires hit Haifa,"24 November 2016. [Online]. Available: 〈http://www.bbc.com/news/world-middle-east-38088651〉. (Accessed 20 December 2016).
[30] N. Spigel, "Haifa Residents Try to Get Back to Normal in a Torched City,"27 November 2016. [Online]. Available: 〈http://www.haaretz.com/israel-news/.premium-1.755464?=&ts=_1482228732506〉. (Accessed 20 December 2016).
[31] Z.B. Begin, Deadly Earthquakes at the Jordan Valley and the Dead Sea – Repetition Periods and Occurrence Probability (Hebrew), Isreali Geological Institute, Jerusalem, 2005.